Original Article

Gynecologic and Obstetric Investigation

Gynecol Obstet Invest 2016;81:193–201
DOI: 10.1159/000431223

Received: January 14, 2015
Accepted after revision: May 6, 2015
Published online: August 26, 2015

Longitudinal Changes in Placental Magnetic Resonance Imaging Relaxation Parameter in Murine Pregnancy: Compartmental Analysis

Uday Krishnamurthy[a, b] Gabor Szalai[c] Yimin Shen[a] Zhonghui Xu[c]
Brijesh Kumar Yadav[a, b] Adi Laurentiu Tarca[c, e] Tinnakorn Chaiworapongsa[c, d]
Edgar Hernandez-Andrade[c, d] Nandor Gabor Than[c, d, h] Ewart Mark Haacke[a, b]
Roberto Romero[c, f, g] Jaladhar Neelavalli[a, b]

[a]Department of Radiology, Wayne State University School of Medicine and [b]Department of Biomedical Engineering, Wayne State University College of Engineering, Detroit, Mich., [c]Perinatology Research Branch, NICHD/NIH/DHHS, Bethesda, Md. and Detroit, Mich., [d]Department of Obstetrics and Gynecology, Wayne State University School of Medicine and [e]Department of Computer Science, Wayne State University, Detroit, Mich., [f]Department of Obstetrics and Gynecology, University of Michigan, Ann Arbor, Mich., and [g]Department of Epidemiology and Biostatistics, Michigan State University, East Lansing, Mich., USA; [h]Institute of Enzymology, Research Centre for Natural Sciences, Hungarian Academy of Sciences, Budapest, Hungary

Key Words

Mouse · Relaxation rate · Spin-spin relaxation · Junctional zone · Labyrinth zone · Relative contribution · High-perfusion zone · Low-perfusion zone

Abstract

Objective: To quantify gestation-dependent longitudinal changes in the magnetic resonance transverse relaxation time (T2) parameter of the major constituent regions of the mouse placenta and to evaluate their relative contributions to changes in overall placental T2. ***Methods:*** Timed-pregnant CD-1 mice underwent magnetic resonance imaging at 7.0 T field strength, on gestational day 13 (GD13), GD15 and GD17. T2 of the placenta and its constituent high and low blood perfusion regions were quantified. A linear mixed-effects model was used to fit the T2 across gestation, and the significance of coefficients was tested. ***Results:*** A decrease in the T2 values of the placenta and its constituent regions was observed across gestation. The temporal change in T2 was estimated to be −1.85 ms/GD ($p < 0.0001$) for the placenta, −1.00 ms/GD ($p < 0.001$) for the high-perfusion zones (HPZs) and −1.66 ms/GD ($p < 0.0001$) for the low-perfusion zones (LPZs). ***Conclusion:*** T2 of the constituent zones of the murine placenta decreases with advancing gestation. While the T2 of the LPZ is smaller than that of the HPZ, there is no difference in their decrease rate relative to that of the whole placenta ($p = 0.24$). The results suggest an increased role of constituent volume fractions in affecting overall gestation-dependent placental T2 decrease in mice.

Parts of the data reported in this paper were presented as a poster at the Joint Annual Meeting of the International Society of Magnetic Resonance in Medicine and the European Society of Magnetic Resonance in Medicine and Biology in Milan, Italy, May 10–16, 2014.

KARGER

© 2015 S. Karger AG, Basel
0378–7346/15/0813–0193$39.50/0

E-Mail karger@karger.com
www.karger.com/goi

Jaladhar Neelavalli, PhD
Department of Radiology, Wayne State University School of Medicine
4201 St. Antoine, Detroit, MI 48201 (USA)
E-Mail jneelava@med.wayne.edu

Roberto Romero, MD, D.Med.Sci
Perinatology Research Branch, NICHD/NIH/DHHS
Wayne State University, Hutzel Women's Hospital
3990 John R Street, Detroit, MI 48201 (USA)
E-Mail romeror@mail.nih.gov

Introduction

Ultrasound (US) is the preferred modality for diagnostic fetal imaging. However, the role of magnetic resonance imaging (MRI) in fetal diagnostic evaluation is increasing in part due to its exquisite soft tissue contrast and its potential to perform quantitative functional imaging [1–4]. US has traditionally been used for fetal screening and assessment mainly due to its ease of operation, high temporal and spatial resolution and adaptability to motion. The choice of prenatal diagnostic imaging (US vs. MRI) is subject to clinical indications [5]. During pregnancy, the placenta plays an important role in the exchange of oxygen and nutrients between the maternal and fetal circulations. Any decline/alteration of this exchange within the placenta is associated with conditions such as intrauterine growth restriction (IUGR) [6, 7]. Experimental studies performed in lamb fetuses have shown that reduced placental blood flow is associated with an increased risk of fetal death and acidosis [8–10]. In human fetuses, increased vascular resistance in the uterine arteries is associated with a higher risk of IUGR and preeclampsia [11, 12], hence placental in vivo assessment plays a crucial role in accessing the health of the fetus. Using MRI it is possible to quantitatively assess the functional and morphological status of the placenta noninvasively [13, 14].

Murine models of pregnancy are extensively used to study placental development due to the anatomical, functional and cellular similarities of the murine and human placentas [15–18]. The mouse placenta consists of three major regions, namely the labyrinth zone, the junctional zone and the decidua. While it is known that the labyrinth zone (analogous to the villous placenta in humans) is the site for maternofetal gas, nutrient and waste exchange, the development of the fetus also depends on the proper functioning of the junctional zone and the decidua [19]. Along with the developing fetus, the placenta shows marked and proportional changes with increasing gestational age (GA), and the different regions of the placenta show differential development [20, 21]. The placenta is subject to continuous structural, morphological and functional changes with advancing gestation. Due to these physiological changes seen across gestation, the quantitative parameters such as volume, capillary density, mass and blood flow are susceptible to normal variation [20, 22, 23]. Hence, characterization of these GA-dependent changes using noninvasive methods is important.

While most placental developmental and structural changes have been studied using stereology or other methods (after euthanizing the fetus) [20, 22], the in vivo assessment of functional development and remodeling of the placenta using noninvasive methods like MRI has been limited. Noninvasive placental blood supply is usually evaluated with Doppler velocimetry (in the uterine arteries), and the placental blood perfusion by calculating three-dimensional power US indices [24–26]. US can also provide information on the size, volume and echogenicity of the placenta [27–29]. Nevertheless placental physiological and functional assessment using US is limited [30, 31]. Of importance, it has been shown that reduced placental volume is accounted for by increased placental efficiency, indicating that functional changes, which often accompany morphological changes, are more physiologically relevant [19, 21]. MRI provides a noninvasive quantitative alternative to functional placental imaging. The MRI transverse relaxation time (T2) parameter has been shown to correlate with microvascular perfusion status of the tissue and is sensitive to changes in perfusion and tissue morphology [32–35]. Quantitative MRI of the placenta, particularly T2, has been shown to be a potential noninvasive biomarker for IUGR in both humans and animal models [36–38]. Conversely, due to normal physiologic changes that occur with aging of the placenta, the T2 parameter may also progressively change with advancing GA [23, 39]. Establishing the trajectory of these normal variations using noninvasive MRI-based methods allows for further use of such methods to recognize changes that occur due to various pathological processes. Furthermore, understanding the normal progression of the T2 of the placenta as a function of gestation could better inform future MRI-based studies for appropriate timing of investigation.

Studies using dynamic contrast-enhanced MRI and contrast-enhanced US have reported distinct functional (perfusion) compartments of the placenta [40, 41]. Placental oxygenation studied using blood oxygen level-dependent MRI under conditions of maternal hyperoxia in humans also suggests distinct compartments [42]. Hence it is imperative to study them independently. These distinct functional compartments of the placenta, the high-perfusion zone (HPZ) and the low-perfusion zone (LPZ), roughly correspond to the labyrinth and the junctional zones. Previous studies have shown that the T2 value of the overall placenta decreases with gestation [23] and that at a given gestation, the T2 values of the constituent placental zones are different [38]. However, it is not clear how the T2 of the constituent zones of the placenta changes with gestation and how they contribute to the GA-dependent decrease of overall placental T2. Therefore, in

this longitudinal study we evaluated the changes in the T2 of the murine placenta and its constituent regions (HPZ and LPZ) at three different time points along the gestational period axis: on gestational day 13 (GD13), GD15 and GD17 (full term duration 19–21 days). An analysis was carried out to evaluate the differential contribution of the individual compartments to the temporal changes in the whole-placenta T2.

Materials and Methods

Animal Care and Handling

The study protocol (A#11-03-11) was approved by the Institutional Animal Care and Use Committee of Wayne State University (Detroit, Mich., USA). Animal care and handling followed the standards set forth by the National Research Council of the National Academies [43] and those published in a previous study [44]. Nine timed-pregnant CD-1 mice were obtained from Charles River Laboratories (Wilmington, Mass., USA). Pregnancy was confirmed by manual examination on GD12. Mice were kept separately in filter top rodent cages and fed with ad libitum water and food. A regular 12:12 h dark-light cycle, constant temperature (24 ± 1°C) and constant humidity (50 ± 5%) were maintained in the animal room, and mice were monitored for food and water intake, vital signs, behavior and activity. MRI was performed on GD13, GD15 and GD17 for each of the nine pregnant mice.

Imaging Procedure

All MRI studies were performed on a 7.0 T, 20 cm bore superconducting magnet (ClinScan; Bruker, Karlsruhe, Germany) interfaced with a Siemens console. Prior to image acquisition, anesthesia was induced by isoflurane to sedate the animals (4% v/v via induction chamber and then 2% v/v maintenance). The mice were kept under anesthesia throughout the acquisition time. The animals were first subjected to a series of localization scans, following which T2-weighted turbo spin echo data were acquired for anatomical assessment of the fetus and high-resolution visualization of the corresponding placentas. A fat-saturated, multi-echo T2-weighted spin echo sequence was used for T2 measurement, which was acquired using the following sequence parameters (table 1): a matrix size of 320 × 512, a repetition time of 2,840 ms, a slice thickness of 0.8 mm, an in-plane resolution of 0.08 × 0.08 mm and a pixel bandwidth of 150 Hz/pixel. A total of six echoes at the echo times (TEs) of 10.8, 21.6, 32.4, 43.2, 54.0 and 64.8 ms were acquired, and T2 maps were generated using a custom code written in MATLAB (The MathWorks Inc., Natick, Mass., USA) for linear least-squares fitting to the mono-exponential signal decay equation [45]:

$$T_2 = -\frac{TE_i - TE_0}{\ln \frac{S_i}{S_0}}.$$

In this equation S_i refers to the magnitude signal intensity at the given TE_i with i = 2, 3, 4, 5, 6, and S_0 and TE_0 refer to the signal and the TE of the first echo, respectively. The data from the six echoes were fitted to this equation to estimate the T2 value. All images were acquired in axial orientation relative to the magnet coordinate system, which was also axial relative to the imaged pregnant mice.

Table 1. MRI parameters used for multi-echo spin echo T2-weighted imaging sequence

Sequence	TE (ms)	TR (ms)	BW (Hz/pixel)	In-plane isotropic voxel size (mm)	Slice thickness (mm)
Multi-echo spin echo	10.8, 21.6, 32.4, 43.2, 54.0, 64.8	2,840	150	0.08×0.08	0.8

BW = Bandwidth; TR = repetition time.

Image Processing

The T2 maps were generated using the multi-echo spin echo data by fitting the signal to a mono-exponential function on a pixel by pixel basis. Pixels with poor fit or those which resulted in negative values were thresholded to zero. A central slice through the placental cross-section, where the constituent HPZ and LPZ were visualized, was chosen for the quantitative T2 measurements. A total of three free-hand-drawn regions of interest (ROIs) were used to map (a) the whole placenta, (b) the HPZ and (c) the LPZ from which the T2 values were recorded. Manual segmentation of the regions was performed considering the spin echo T2-weighted images at different TEs, primarily the data at TEs of 32.4, 43.2 and 54.0 ms as they are closest to the whole-placental T2 values previously reported [23], providing good T2 contrast. The ROIs for the HPZ and LPZ were drawn conservatively to avoid partial volume voxels at the boundaries of these regions. The whole-placenta ROI was drawn to include the high- and low-perfusion regions along with the boundary regions that could not be definitively classified into either of these two regions. A minimum of 40 voxels were included in the ROIs to ensure low standard error in the mean T2 measurement. The decidua was not included in the whole-placenta ROI. Longitudinal changes in the placental T2 values were then statistically compared for differences. Since maternal systemic blood pressure and heart rate increase during murine pregnancies [46], such systemic differences in maternal physiology due to advancement in pregnancy could act as a confounding factor influencing the placental T2 measure. Systemic changes in maternal cardiovascular physiology are expected to affect T2 values of maternal organs like muscle. Therefore, the changes in T2 value of maternal muscle tissue, specifically the lateral group of muscles of the hind limb, as a function of GA were statistically evaluated.

Statistical Analysis

The T2 measurements from different placentas in a given mice on a given GD were averaged. The averaged T2 values were evaluated for possible changes due to advancing gestation. The linear temporal patterns across GA for T2 measurements were fitted using a linear mixed-effects (LME) model. The fixed effects included GD as a continuous variable, T2 measurements from a given com-

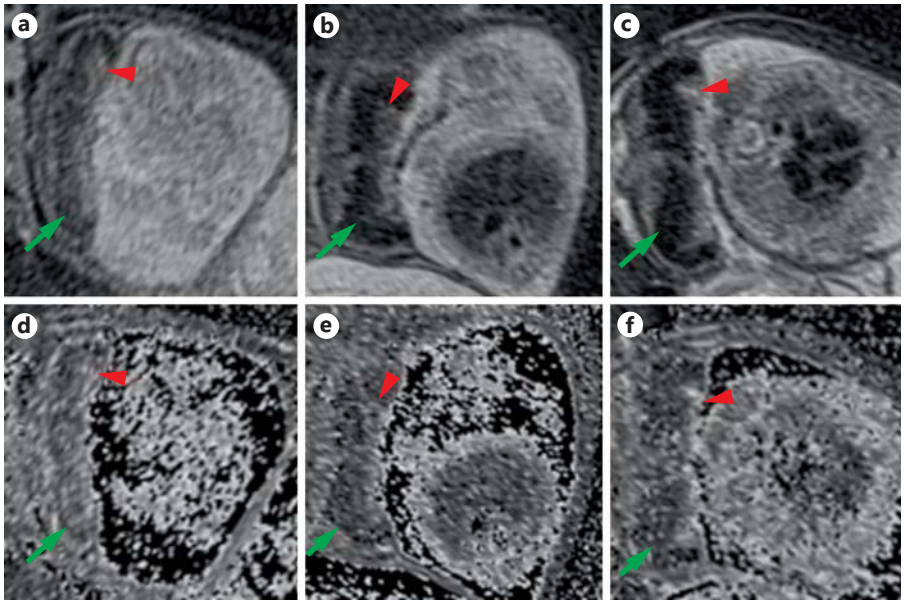

Color version available online

Fig. 1. T2 maps of the murine placenta shown across different GAs. **a–c** T2-weighted images of the murine placenta on GD13 (**a**), GD15 (**b**) and GD17 (**c**). **d–e** Quantitative T2 maps of the corresponding placenta are also shown. Note the contrast between the two constituent regions (HPZ: red arrowheads; LPZ: green arrows; colors refer to the online version only).

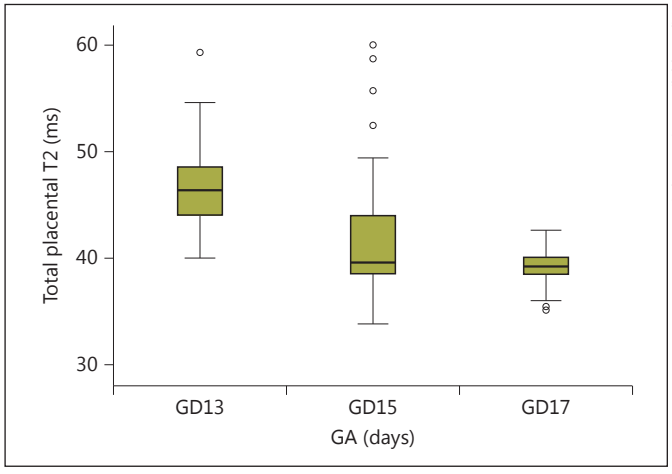

Color version available online

Fig. 2. T2 murine placental transverse relaxation times at different GAs. T2 transverse relaxation times of the murine placenta on GD13, GD15 and GD17 are represented in ms.

Table 2. Transverse relaxation time (T2, ms, mean ± SD) of the individual compartments of the placenta across different GDs

GD	Whole placenta		HPZ		LPZ	
	mean	SD	mean	SD	mean	SD
13	46.23	4.20	60.76	4.07	40.67	3.74
15	42.19	6.60	59.85	5.77	37.13	5.67
17	39.08	1.67	56.50	3.68	34.12	1.99

SD = Standard deviation.

partment (total placenta, HPZ, LPZ) and the interaction between these two variables, and a random intercept was exercised for each mouse. Furthermore, the presence or absence of systematic changes in maternal physiology was ascertained by statistically evaluating changes in the T2 value of the reference maternal muscle tissue as a function of GA using a repeated measures analysis of variance test. All visualization and analysis were performed within the R computing environment [47], and the LME model was built using R package 'nlme' [48].

Results

T2 Relaxation Times

The placental T2 relaxation times decreased with advancing gestation (table 2). A total of nine mice were followed longitudinally. T2 values were measured from a total of 35 placentas on GD13, from 36 placentas on GD15 and from 35 placentas on GD17. The T2-weighted images showed the clear distinction of the constituent regions of the placenta (fig. 1). The average whole-placenta T2 relaxation time, measured across all placentas, was 46.23 ± 4.2 ms (mean ± standard deviation) on GD13, 42.19 ± 6.60 ms on GD15 and 39.08 ± 1.67 ms on GD17 (fig. 2). Here, the standard deviations represent the variation of the measured T2 value from one placenta to another. The standard error in individual T2 measures from a given ROI did not exceed 0.3 ms across all placentas evaluated. The average T2 value for the HPZ, measured across all placentas, was 60.76 ± 4.07 ms on GD13, 59.85 ± 5.77 ms on GD15 and 56.50 ± 3.68 ms on GD17. The

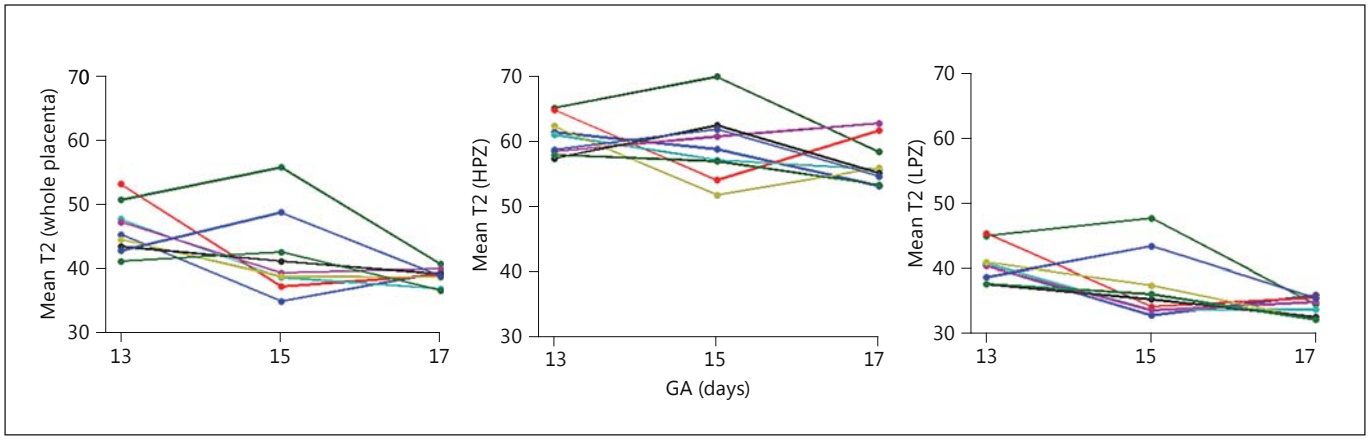

Fig. 3. Time course plots of the averaged T2 transverse relaxation time across different regions of the placenta. Time course plots of the averaged T2 transverse relaxation time across the whole placenta (left), the HPZ (middle) and the LPZ (right). Each point corresponds to the average T2 of all placentas of mice at a given GA. The different colors indicate different mice that were longitudinally followed (colors refer to the online version only).

corresponding average T2 value for the LPZ was 40.67 ± 3.74 ms on GD13, 37.13 ± 5.67 ms on GD15 and 34.12 ± 1.99 ms on GD17.

The three T2 values from a given mouse (whole placenta, HPZ and LPZ) over all the placentas at a given GD were averaged. Then a global LME model was built for these averaged T2 values with fixed effects including GD as a continuous linear predictor, the T2 values as a factor predictor and their interactions. From this model, the rate of T2 temporal change was estimated to be –1.85 ms/GD ($p = 4.36 \times 10^{-6}$) for the whole placenta, –1.00 ms/GD ($p = 8.73 \times 10^{-3}$) for the HPZ and –1.66 ms/GD ($p = 3.12 \times 10^{-5}$) for the LPZ (fig. 3). However, overall there was no significant difference among the three rates ($p = 0.24$). In particular, the difference between the rates of HPZ T2 and placental T2 was 0.85 ($p = 0.11$), and the difference between the rates of LPZ T2 and placental T2 was 0.197 ($p = 0.71$). Though not significant, the linear trend of placental T2 was closer to that of LPZ T2.

The influence of maternal systemic changes was evaluated by analyzing the changes in maternal muscle T2 across the three GDs. A repeated measure single factor analysis of variance with Greenhouse-Geisser correction showed that the mean T2 values of maternal muscle were similar across the three GDs ($p = 0.76$). This invariance of maternal muscle T2 across different GDs indicates that the GD-dependent change observed in the placental T2 values was not influenced by systemic changes in maternal physiology with advancing gestation.

Discussion

The principal findings of the study were as follows: (1) Placental T2 values decrease with advancing gestation in normal murine pregnancy. (2) T2 values of both the HPZ and the LPZ decrease with gestation, the T2 value of LPZ being lower than that of the HPZ. (3) The slope of linear decrease in T2 with GA for the whole placenta is closer to that of the LPZ than to that of the HPZ, although there is no significant difference among the trends for the three (HPZ, LPZ and whole placenta).

Our findings of a longitudinal decrease in the T2 relaxation parameter of the overall placenta with advancing GA are similar to those observed in the human placenta [36, 39]. In murine placenta, while a previous report quantified overall placental T2 in a cross-sectional cohort [23], this is the first study reporting longitudinal T2 changes in the constituent zones of the murine placenta. The constituent functional zones of the placenta have been referred to as high- and low-perfusion regions in this work based on features observed in contrast-enhanced studies reported in the mouse placenta [41, 49]. The high-perfusion region roughly corresponds to the labyrinth zone and the low-perfusion region to the junctional zone [41, 49].

The MRI relaxation parameter, T2, of a tissue depends on multiple parameters, including presence of magnetic field-perturbing inclusions like deoxygenated red blood cells and their volume fraction within the tissue [50]. T2 also depends on the diffusion characteristics

of tissue water (restricted vs. freely diffusing). The equation that tersely summarizes these dependencies is given in [50–52]:

$$T_2 \propto \frac{1}{v \cdot (\Delta\omega)^2 \cdot D^a}.$$

Here, D is the diffusion coefficient of tissue water content, v is the tissue volume fraction of the susceptibility inclusions that perturb the magnetic field, like deoxyhemoglobin (e.g. blood volume fraction); $\Delta\omega$ is the parameter characterizing the magnitude of field perturbation from the susceptibility inclusions, which inversely relates to blood oxygen saturation. The exponent α depends on the physical nature of water diffusion in the tissue, restricted versus unrestricted [51]. The placenta is a highly vascularized organ containing both oxygenated and deoxygenated blood. A decrease in T2 observed in the whole placenta as well as its constituent functional compartments as a function of GA could be due to a change in one or more of these three tissue characteristics: (a) blood volume fraction *(v)*, (b) decreased oxygen saturation (i.e. decrease in $1/\Delta\omega$), or (c) an increase in tissue water diffusion *(D)*. The placental capillary density in mice is known to increase with advancing gestation, with a corresponding increase in capillary surface area to volume ratio [22, 53], thus increasing v. This increase in blood volume fraction could lead to a corresponding decrease in T2, assuming that the other parameters of water diffusion *(D)* and blood oxygenation levels ($1/\Delta\omega$) remain the same. When compared with the literature, however, the percent decrease in the T2 values observed in either the HPZ or the overall placenta in this study is much less than the percent increase in the placental blood volume fraction reported [20, 53]. For example, an increase of 22% in blood volume fraction of the labyrinth zone was observed at GD17.5 relative to GD15.5 by Rennie et al. [53]. The corresponding percent decrease in T2 of the HPZ observed in this study was only 5.6%. This indicates that the change in blood volume fraction may be accompanied by concomitant changes in the other parameters ($1/\Delta\omega$ and D) that affect T2. This is conceivable since the thickness of the interhemal membrane, which influences water diffusion between maternal and fetal blood spaces, also decreases with gestation [20, 53], leading to a theoretical increase in diffusion capacity (diffusion coefficient, D) with gestation [20]. Recent MRI-based reports on the placental apparent diffusion coefficient, a measure of water diffusion in the whole placenta, however, showed no significant change with advancing gestation in either humans or mice [54, 55]. While these studies use relatively low-resolution imaging and pertain to whole-placenta diffusion, a region-specific study of diffusion characteristics within the placenta, for example labyrinth versus junctional, could help us in better observing their change trajectory as a function of GA. Lastly, how the parameter $1/\Delta\omega$, which is proportional to blood oxygenation, changes with advancing gestation within the whole placenta or in its constituent regions is unclear. Interestingly, a recent study in rats showed an increased percent change in T2* (a parameter proportional to T2) of the HPZ compared to the LPZ under maternal hyperoxygenation [56], indicating different baseline blood oxygenation levels in these compartments. Nevertheless, further studies quantifying blood oxygenation ($1/\Delta\omega$) of the constituent zones and its changes with advancing gestation are required. Quantitative susceptibility mapping techniques may have a role to play in such studies as they allow for noninvasive quantification of in vivo blood oxygenation [57–59].

On all the three GDs investigated, we found that the T2 value of the HPZ (labyrinth) is higher than that of the LPZ (junctional). The junctional zone (LPZ) in the murine placenta principally consists of spongiotrophoblasts lining the venous sinuses that contain deoxygenated maternal blood draining the labyrinth zone of the placenta [60, 61]. On the other hand, the labyrinth zone (HPZ) is the principal maternal-fetal exchange zone. Thus, while the labyrinth zone (HPZ) contains both oxygenated and deoxygenated blood fractions from the maternal and fetal circulation, the junctional zone (LPZ) predominantly contains predominantly deoxygenated blood. Consequently, the $1/\Delta\omega$ parameter (proportional to blood oxygenation) has a lower value in the junctional zone (LPZ) compared to the labyrinth zone (HPZ). This could explain the shorter T2 observed in the LPZ, in addition to the presence of glycogen-rich cells [62]. Though not significant, the T2 change as a function of GA of the LPZ (–1.66 ms/GD) was closer to that of the whole placenta (–1.85 ms/GD) compared to the HPZ (–1.0 ms/GD). The higher slope of the whole placental T2 can be attributed to the differential increase in the volume of the constituent regions [20, 49].

The ratio of the absolute T2 of HPZs to LPZs ($T2_{\text{high perfusion}}/T2_{\text{low perfusion}}$ corresponding to $T2_{\text{labyrinth}}/T2_{\text{junctional}}$) at GD17 was found to be 1.7 in our study. In comparison, a cross-sectional study in mice reported this ratio to be 2.5 (at GD17.5) [38]. This difference could largely be attributed to the magnetic strength at which imaging was carried out (7.0 T in our study vs. 11.74 T). Other factors leading to this difference could include the

different strain of the mice studied (CD-1 in our study vs. C57BL/6JArc) and differences in imaging resolution (i.e. effect of partial voluming). Furthermore, the T2 of blood decreases quadratically with magnetic field strength [63, 64], which in turn could differentially affect the T2 value of placental tissue, depending on the extent of its vascular density and oxygen saturation.

Systemic maternal cardiovascular factors could, in principle, influence the T2 values measured in the placenta. However, no significant change in maternal muscle tissue as a function of GA was observed in this study, indicating that maternal physiology did not change with GA, and our observations on alterations in T2 were due to placental developmental changes. Due to the functional dependence of T2 relaxation on parameters like blood oxygenation status, vascular density, volume and water diffusion in tissue [37, 51], it has been found to be a significant parameter for the diagnosis of preeclampsia and IUGR [39]. However, the role of each of these functional parameters and their natural progression across gestation continues to be an active area of research. In pregnancies complicated by preeclampsia and IUGR, studies have demonstrated shorter placental T2 relaxation times [39, 65]. In this context, it becomes important to understand the physiological decrease in the relaxation time that can be attributed to GA. The results presented in this study quantify this change. Different regions of the placenta show differential development with progressing gestation [19] and thus might be affected differently when there is placental pathology. Hence, regional analysis of the T2 parameter was carried out in this study.

There are a few limitations to this study. The LME model used for the analysis assumes a linear relation between the T2 parameter and GA; the use of a nonlinear model with a greater sample size across many GDs might increase the sensitivity of the quantitative MRI parameter. T2 measurements from the central slices of the placenta were used in this study with conservative ROI placements within constituent placental regions. During longitudinal scans of the same pregnant mice, identifications of the same set of placentas and fetuses between different GDs were not possible and remain a practical challenge [66]. Hence, the average data from a group of placentas, evaluated longitudinally, is presented. Nevertheless, this aspect should not affect the conclusions of this study because, despite some placenta-to-placenta variation of the measured T2 parameter, the changes with GA in both the placenta and its constituent regions were found to be significant.

Conclusions

Placental T2 relaxation times decrease with advancing gestation in murine pregnancy. A significant decrease in T2 values of the constituent HPZs and LPZs of the placenta is also observed and the T2 value of the LPZ is smaller than that of the HPZ across gestation. The absolute T2 value of LPZ is closer to that of the whole placenta. Furthermore, while not statistically significant, the slope of the T2 versus GA curve for the LPZ (as opposed to the HPZ) was closer to that observed in the whole placenta. These results indicate the increased role of the respective volume fractions of these constituent zones influencing the overall placental T2 versus GA trajectory.

Acknowledgements

This research was supported, in part, by the Perinatology Research Branch, Division of Intramural Research, Eunice Kennedy Shriver National Institute of Child Health and Human Development (NICHD), National Institutes of Health (NIH), Department of Health and Human Services (DHHS) and, in part, by federal funds from NICHD (NIH, DHHS) under contract No. HHSN275201300006C. The authors are grateful to Dr. Theodore Price (Perinatology Research Branch), Dr. Lisa J. Brossia-Root, Laura Lee McIntyre and all personnel involved in the Division of Laboratory Animal Resources (Wayne State University). This research and the writing of the manuscript was also supported in part by a Small Business Technology Transfer (STTR) grant from the National Heart, Lung, and Blood Institute (NHLBI, NIH, DHHS; 1R42HL112580-01A1), by Wayne State University's Perinatal Research Initiative and Perinatology Virtual Discovery Grant to J. Neelavalli (made possible by the W.K. Kellogg Foundation award P3018205). U. Krishnamurthy was the recipient of a Thomas C. Rumble fellowship from Wayne State University. N.G. Than is the recipient of a Hungarian Academy of Sciences Momentum Grant (#LP2014-7/2014).

Disclosure Statement

The authors have no conflicts of interest.

References

1 Levine D: Ultrasound versus magnetic resonance imaging in fetal evaluation. Top Magn Reson Imaging 2001;12:25–38.

2 Duncan K, Baker P, Johnson I: The complementary role of echoplanar magnetic resonance imaging and three-dimensional ultrasonography in fetal lung assessment. Am J Obstet Gynecol 1997;177:244–245.

3 Malinger G, Lev D, Lerman-Sagie T: Is fetal magnetic resonance imaging superior to neurosonography for detection of brain anomalies? Ultrasound Obstet Gynecol 2002;20:317–321.

4 Meyer-Wittkopf M, et al: Evaluation of three-dimensional ultrasonography and magnetic resonance imaging in assessment of congenital heart anomalies in fetal cardiac specimens. Ultrasound Obstet Gynecol 1996;8:303–308.
5 Pugash D, et al: Prenatal ultrasound and fetal MRI: the comparative value of each modality in prenatal diagnosis. Eur J Radiol 2008;68:214–226.
6 Baschat AA: Fetal responses to placental insufficiency: an update. BJOG 2004;111:1031–1041.
7 Baschat AA: Pathophysiology of fetal growth restriction: implications for diagnosis and surveillance. Obstet Gynecol Surv 2004;59:617–627.
8 Lang U, et al: Fetal umbilical vascular response to chronic reductions in uteroplacental blood flow in late-term sheep. Am J Obstet Gynecol 2002;187:178–186.
9 Lang U, et al: Effects of chronic reduction in uterine blood flow on fetal and placental growth in the sheep. Am J Physiol Regul Integr Comp Physiol 2000;279:R53–R59.
10 Rees S, et al: Fetal brain injury following prolonged hypoxemia and placental insufficiency: a review. Comp Biochem Physiol A Mol Integr Physiol 1998;119:653–660.
11 Aardema MW, et al: Uterine artery Doppler flow and uteroplacental vascular pathology in normal pregnancies and pregnancies complicated by pre-eclampsia and small for gestational age fetuses. Placenta 2001;22:405–411.
12 Campbell S, et al: Qualitative assessment of uteroplacental blood flow: early screening test for high-risk pregnancies. Obstet Gynecol 1986;68:649–653.
13 Linduska N, et al: Placental pathologies in fetal MRI with pathohistological correlation. Placenta 2009;30:555–559.
14 Francis ST, et al: Non-invasive mapping of placental perfusion. Lancet 1998;351:1397–1399.
15 Georgiades P, Ferguson-Smith AC, Burton GJ: Comparative developmental anatomy of the murine and human definitive placentae. Placenta 2002;23:3–19.
16 Rossant J, Cross JC: Placental development: lessons from mouse mutants. Nat Rev Genet 2001;2:538–548.
17 Watson ED, Cross JC: Development of structures and transport functions in the mouse placenta. Physiology (Bethesda) 2005;20:180–193.
18 Dilworth MR, Sibley CP: Review: Transport across the placenta of mice and women. Placenta 2013;34(suppl):S34–S39.
19 Coan PM, et al: Adaptations in placental nutrient transfer capacity to meet fetal growth demands depend on placental size in mice. J Physiol 2008;586:4567–4576.
20 Coan PM, Ferguson-Smith AC, Burton GJ: Developmental dynamics of the definitive mouse placenta assessed by stereology. Biol Reprod 2004;70:1806–1813.
21 Mayhew TM: Allometric studies on growth and development of the human placenta: growth of tissue compartments and diffusive conductances in relation to placental volume and fetal mass. J Anat 2006;208:785–794.
22 Rennie MY, et al: 3D visualisation and quantification by microcomputed tomography of late gestational changes in the arterial and venous feto-placental vasculature of the mouse. Placenta 2007;28:833–840.
23 Krishnamurthy U, et al: Quantitative T2 changes and susceptibility-weighted magnetic resonance imaging in murine pregnancy. Gynecol Obstet Invest 2014;78:33–40.
24 Espinoza J, et al: Normal and abnormal transformation of the spiral arteries during pregnancy. J Perinat Med 2006;34:447–458.
25 Welsh AW, et al: Development of three-dimensional power Doppler ultrasound imaging of fetoplacental vasculature. Ultrasound Med Biol 2001;27:1161–1170.
26 Jones NW, et al: Placental 3-D power Doppler angiography – regional variation and reliability of two ultrasonic sphere biopsy techniques. Ultrasound Med Biol 2011;37:364–375.
27 Odibo AO, et al: Placental volume and vascular flow assessed by 3D power Doppler and adverse pregnancy outcomes. Placenta 2011;32:230–234.
28 Milligan N, et al: Two-dimensional sonographic assessment of maximum placental length and thickness in the second trimester: a reproducibility study. J Matern Fetal Neonatal Med 2014, Epub ahead of print.
29 Kusanovic JP, et al: Discordant placental echogenicity: a novel sign of impaired placental perfusion in twin-twin transfusion syndrome? J Matern Fetal Neonatal Med 2010;23:103–106.
30 Sarmandal P, Grant JM: Effectiveness of ultrasound determination of fetal abdominal circumference and fetal ponderal index in the diagnosis of asymmetrical growth retardation. Br J Obstet Gynaecol 1990;97:118–123.
31 Falo AP: Intrauterine growth retardation (IUGR): prenatal diagnosis by imaging. Pediatr Endocrinol Rev 2009;6(suppl 3):326–331.
32 An H, et al: Evaluation of MR-derived cerebral oxygen metabolic index in experimental hyperoxic hypercapnia, hypoxia, and ischemia. Stroke 2009;40:2165–2172.
33 Silvennoinen MJ, et al: Comparison of the dependence of blood R2 and R2* on oxygen saturation at 1.5 and 4.7 Tesla. Magn Reson Med 2003;49:47–60.
34 Kavec M, et al: Use of spin echo T(2) BOLD in assessment of cerebral misery perfusion at 1.5 T. MAGMA 2001;12:32–39.
35 Cieszanowski A, et al: Discrimination of benign from malignant hepatic lesions based on their T2-relaxation times calculated from moderately T2-weighted turbo SE sequence. Eur Radiol 2002;12:2273–2279.
36 Wright C, et al: Magnetic resonance imaging relaxation time measurements of the placenta at 1.5 T. Placenta 2011;32:1010–1015.
37 Derwig I, et al: Association of placental T2 relaxation times and uterine artery Doppler ultrasound measures of placental blood flow. Placenta 2013;34:474–479.
38 Bobek G, et al: Magnetic resonance imaging detects placental hypoxia and acidosis in mouse models of perturbed pregnancies. PLoS One 2013;8:e59971.
39 Duncan KR, et al: The investigation of placental relaxation and estimation of placental perfusion using echo-planar magnetic resonance imaging. Placenta 1998;19:539–543.
40 Zhou YJ, et al: Real-time placental perfusion on contrast-enhanced ultrasound and parametric imaging analysis in rats at different gestation time and different portions of placenta. PLoS One 2013;8:e58986.
41 Remus CC, et al: Application of the steepest slope model reveals different perfusion territories within the mouse placenta. Placenta 2013;34:899–906.
42 Sorensen A, et al: Changes in human placental oxygenation during maternal hyperoxia estimated by blood oxygen level-dependent magnetic resonance imaging (BOLD MRI). Ultrasound Obstet Gynecol 2013;42:310–314.
43 Guide for the Care and Use of Laboratory Animals, ed 8. Washington, The National Academies Press, 2011.
44 Szalai G, et al: In vivo experiments reveal the good, the bad and the ugly faces of sFlt-1 in pregnancy. PLoS One 2014;9:e110867.
45 Haacke EM, et al: Magnetic Resonance Imaging. New York, Wiley-Liss, 1999.
46 Wong AY, et al: Maternal cardiovascular changes during pregnancy and postpartum in mice. Am J Physiol Heart Circ Physiol 2002;282:H918–H925.
47 R Development Core Team: R: A Language and Environment for Statistical Computing. Vienna, R Foundation for Statistical Computing, 2013.
48 Pinheiro J, et al: nlme: linear and nonlinear mixed effects models. R package version 3.1-108. Vienna, R Foundation for Statistical Computing, 2013. http://cran.r-project.org/web/packages/nlme/ (accessed February 2013).
49 Yadav BK, Krishnamurthy UB, Shen Y, Szalai G, Neelavalli J, Wang B, Chaiworapongsa T, Hernandez-Andrade E, Than NG, Haacke EM, Romero R: Evaluating placental growth in normal murine pregnancy using tissue-similarity-mapping and dynamic contrast enhanced magnetic resonance imaging. Joint Annual Meeting of the ISMRM-ESMRMB, Milan, 2014.
50 Jensen J, Chandra R: NMR relaxation in tissues with weak magnetic inhomogeneities. Magn Reson Med 2000;44:144–156.
51 Gossuin Y, Gillis P, Lo Bue F: Susceptibility-induced T(2)-shortening and unrestricted diffusion. Magn Reson Med 2002;47:194–195.

52 Brooks RA, Moiny F, Gillis P: On T2-shortening by weakly magnetized particles: the chemical exchange model. Magn Reson Med 2001; 45:1014–1020.
53 Rennie MY, et al: Expansion of the fetoplacental vasculature in late gestation is strain dependent in mice. Am J Physiol Heart Circ Physiol 2012;302:H1261–H1273.
54 Solomon E, et al: Major mouse placental compartments revealed by diffusion-weighted MRI, contrast-enhanced MRI, and fluorescence imaging. Proc Natl Acad Sci USA 2014; 111:10353–10358.
55 Sivrioğlu AK, et al: Evaluation of the placenta with relative apparent diffusion coefficient and T2 signal intensity analysis. Diagn Interv Radiol 2013;19:495–500.
56 Chalouhi GE, et al: Fetoplacental oxygenation in an intrauterine growth restriction rat model by using blood oxygen level-dependent MR imaging at 4.7 T. Radiology 2013;269:122–129.
57 Haacke EM, et al: Susceptibility mapping as a means to visualize veins and quantify oxygen saturation. J Magn Reson Imaging 2010;32: 663–676.
58 Neelavalli J, et al: Measuring venous blood oxygenation in fetal brain using susceptibility-weighted imaging. J Magn Reson Imaging 2014;39:998–1006.
59 Fan AP, et al: Regional quantification of cerebral venous oxygenation from MRI susceptibility during hypercapnia. Neuroimage 2015; 104:146–155.
60 Coan P, Ferguson-Smith A, Burton G: Ultrastructural changes in the interhaemal membrane and junctional zone of the murine chorioallantoic placenta across gestation. J Anat 2005;207:783–796.
61 Adamson SL, et al: Interactions between trophoblast cells and the maternal and fetal circulation in the mouse placenta. Dev Biol 2002; 250:358–373.
62 Coan PM, et al: Origin and characteristics of glycogen cells in the developing murine placenta. Dev Dyn 2006;235:3280–3294.
63 Gossuin Y, Muller RN, Gillis P: Relaxation induced by ferritin: a better understanding for an improved MRI iron quantification. NMR Biomed 2004;17:427–432.
64 Brooks RA, et al: Comparison of T2 relaxation in blood, brain, and ferritin. J Magn Reson Imaging 1995;5:446–450.
65 Gowland P, et al: In vivo relaxation time measurements in the human placenta using echo planar imaging at 0.5 T. Magn Reson Imaging 1998;16:241–247.
66 Avni R, et al: Unique in utero identification of fetuses in multifetal mouse pregnancies by placental bidirectional arterial spin labeling MRI. Magn Reson Med 2012;68:560–570.